A Fully 3D Maximum Likelihood Estimator Algorithm with Attenuation and Scatter Correction Adapted to a Limited Angle Positron Camera

F. Pönisch[1], W. Enghardt[1], K. Lauckner[2]
[1]Forschungszentrum Rossendorf, Postfach 510119, 01314 Dresden, Germany
[2]Scientific Consulting Group GmbH, Bismarckallee 9, 79098 Freiburg, Germany

Abstract—**The in beam dual head positron camera BASTEI (Beta$^+$ Activity meaSurements at the Therapy with Energetic Ions) is used to monitor and control the applied dose distributions simultaneously to tumour irradiations with carbon ion beams at the experimental heavy ion therapy facility at GSI Darmstadt. Therefore, the PET system has been mounted directly at the treatment site. A fully 3D reconstruction algorithm based on the Maximum Likelihood Estimator algorithm has been developed and adapted to a strongly spatial varying imaging situation. The scatter and attenuation correction is applied to the measured list mode data before each iterative step. This requires an attenuation map containing the information on the tissue composition and densities. This information is derived from the X-ray computed tomograms (CT) of the patient and the patient fixation system including the head rest. The scatter correction method uses the subtraction of calculated scattered from measured data. The normalization of scattered events relative to the unscattered events is done by a global scatter fraction factor. The results are presented.**

1. INTRODUCTION

Since 1997 85 patients mainly suffering from head and neck tumours have been treated at the experimental heavy ion tumour therapy facility at GSI Darmstadt. The carbon ion therapy is favourable for treating compact, radioresistant tumours in close vicinity of organs at risk. Therefore, a dedicated in-beam PET system has been built. During the irradiation β^+-radioactive nuclei are produced by nuclear fragmentation reactions along the path of the beam. This activity can be related to the original dose distribution and imaged in-situ by means of positron emission tomography. The dedicated positron camera BASTEI has been integrated into the treatment facility, it has a dual-head geometry in order to avoid interference with the horizontally fixed beam and restrictions to the patient positioning [1]. The two large-area detector heads, which have been assembled from components of the ECAT EXACT® PET-scanner, are mounted above and below the patient couch. The measured list mode data are reconstructed by a fully 3D noise suppressing Maximum Likelihood algorithm.

Furthermore, the expected counting statistics is limited by the doses applied per therapy fraction and is usually two to three orders of magnitude lower compared with those of typical PET-scans in nuclear medicine. Nevertheless, the rather simple shape of the activity distributions alleviates the reconstruction problem.

The individual detector response of the 4 Mio. lines of response (LOR) are corrected by means of a normalisation scan. It is performed with a line source moving through the field of view (FOV) of the camera.

The process of photon scattering considerably influences the image quality in PET. For head and neck tumours about 20 % of the registered true coincidences are influenced by Compton or Rayleigh scattering, which may destroy the correspondence between the source and the reconstructed radioactivity distribution especially in highly inhomogeneous regions of the human body.

2. IMPLEMENTATION

Since the β^+-activity distribution is well localized to the irradiated volume, the scatter correction algorithm requires the information on the tissue composition and density only within and nearby the camera FOV. This is derived from the X-ray CT of the patient (created for treatment planning purpose) which is automatically combined with a CT of the head rest (Fig. 1) using characteristic landmarks. The created data set is the basis for the calculation of the attenuation correction factors. The correct position of these CTs with respect to the positron camera is derived from stereotactic coordinates used during the diagnostic CT scan and for patient positioning before the irradiation. The Fig. 1 shows the significant influence of the absorption by the head rest on the detector response leading, if not corrected, to image artefacts in the reconstruction. The dashed line denotes the acceptance cone of the tomograph

.

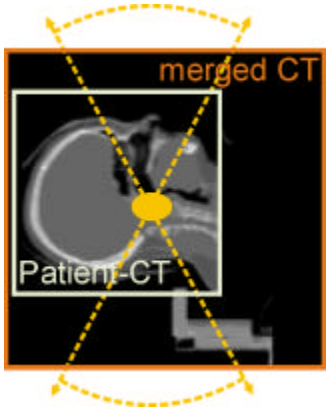

Figure 1: The density distribution used for attenuation and scatter correction obtained from the patient CT and from the CT of the patient support. A typical tumour location and the acceptance cone of the positron camera are displayed.

The reconstruction is based on the Maximum Likelihood Estimation algorithm [2] and has been extended to a three dimensional image space [3]:

$$x_j^{(n+1)} = x_j^{(n)} \cdot \sum_i \frac{a_{ij} y_i^{*(n)}}{\sum_{j'} a_{ij} x_{j'}^{(n)}} \qquad (1)$$

$x_j^{(n)}$ denotes the activity distribution after the n-th iteration step, $y_i^{*(n)}$ is the modified measured projection for the i-th LOR and a_{ij} is the element of the transition matrix.

The aim was to model the above described non-standard imaging situation as accurate as possible within an acceptable computation time. The reconstruction is performed by using an image space with a size adapted to the irradiated volume (typical image size of 0.5 million voxels with a size of 1.6875 mm). During the treatment with a typical physical dose of 0.8 Gy per fraction around 100,000 coincidences are acquired.

The non-zero elements of the transition matrix required for a particular reconstruction are calculated at run time. In order to consider the individual crystal response, the volume of each LOR is sampled by 10 lines whose endpoints are randomly distributed over the crystal volume taking into account the interaction probability depending exponentially on the depth of interaction and the spatial orientation of the crystals. The following pre-iterative correction for each coincidence channel i are applied:

$$y_i^{meas} = (y_i^p - y_i^r) \cdot \frac{w_i^p}{w_i^e} \qquad (2)$$

where y_i^p and y_i^r denotes the number of the measured prompt and random coincidences, respectively. The correction factor w_i^p depends on the length of the emission line within the image space divided by the total length of the longitudinal image space axis whereas w_i^e is the detection efficiency.

The scatter correction is applied to the measured projections before each iteration step. Thus, the events registered for LOR i (y_i^{meas}) can be considered as the sum of the unscattered events from this LOR ($y_i^{unscatt}$) and of events scattered into this LOR from outside (y_i^{scatt}):

$$y_i^{meas} = y_i^{unscatt} + y_i^{scatt} . \qquad (3)$$

The correction step of equation (1) has to be performed for the unscattered and attenuation corrected events, i.e.:

$$y_i^{*(n)} = \frac{y_i^{unscatt}}{a_i} = \frac{y_i^{meas} - y_i^{scatt}}{a_i} , \qquad (4)$$

where a_i is the total attenuation along LOR i.

To calculate the quantity y_i^{scatt} we follow the approximation of Ollinger [4] and Watson [5] denoted as the Single Scatter Simulation (SSS). This algorithm approximates the scatter coincidences in a given LOR by single Compton scattered events only. At first, a sample of around 1000 scatter points S is randomly distributed throughout the scatter volume where the density exceeds 0.1 g/cm^3 (Hounsfield > -900).

Figure 2 shows a LOR labelled *AB*. For each scatter point S there will be two distinct contributions to the single scattered coincidences, depending on which side of the scatter point the annihilation takes place (Q_1, Q_2).

The first addend in equation (6) supposes that the annihilation takes place at a point Q_1 between S and A. The photon which reaches the crystal A is unscattered. The scatter contribution for *AB* is calculated according to the following formula in a discrete notation:

$$y_i' = \sum_S \sum_{j \in AS} x_j^{(n)} \cdot e^{-\int_A^S \mu(E,s)ds} \cdot \frac{dP_{sc}(\theta(S))}{d\Omega} \cdot \Omega_{detB} \cdot e^{-\int_S^B \mu(E',s)ds} + A \leftrightarrow B \qquad (5)$$

In this expression μ is the linear attenuation coefficient (derived from the merged CT), E and E' denote the photon energy before and after the Compton scatter, respectively, depending on the scatter angle θ, $\frac{dP_{sc}(\theta(S))}{d\Omega}$ is the probability of Compton scatter by the angle θ from S into B and Ω_{detB} is the solid angle of the detector relative to S.

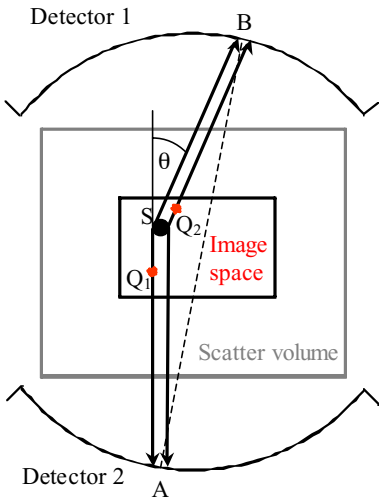

Figure 2: Trajectories of scattered photons

The total number of scattered events calculated

$$N_u^{scatt} = \sum_i y_i' \qquad (6)$$

has to be normalized to the number of acquired coincidences. Because of the limited angle geometry and the low counting statistics it is impossible to apply the normalization procedure according to Watson [5] which based on a scatter rate estimation from measured data. As an alternative we calculate by means of an additional Monte Carlo simulation the global scatter fraction SF from the n-th solution:

$$SF = \frac{N_{scatt}}{N_{true} + N_{scatt}} = \frac{N_{scatt}}{N_{meas}} \qquad (7)$$

where

$$N_{scatt} = \sum_i y_i^{scatt}, \quad N_{meas} = \sum_i y_i^{meas} .$$

From this follows:

$$y_i^{scatt} = y_i' \cdot \frac{SF \cdot N_{meas}}{N_u^{scatt}} . \qquad (8)$$

Introducing eq. (8) into eq. (4) yields the projection value $y_i^{*(n)}$ for each iteration step.

3. RESULTS

The algorithm has been validated using point-like ^{22}Na in a water filled cylindrical phantom (diameter 15 cm, height 15 cm).

Several geometrical configurations were simulated by means of Monte Carlo and reconstructed with the new scatter correction algorithm.

The reconstruction algorithm has been applied successfully to patient data. In dependence on the number of measured coincidences that contribute to the image space, the reconstruction time varies between 120 and 240 minutes on a R8000 processor (75 MHz) of an SGI Power Challenge. The faster converging algorithm OSEM is taken into account, but not implemented up to now.

4. REFERENCES

[1] J. Pawelke et al., "The investigation of different cameras for in-beam PET imaging", *Phys. Med. Biol.* vol. 41, pp. 279-296, 1996

[2] L.A. Shepp, Y. Vardi, "Maximum Likelihood reconstruction for emission tomography", *IEEE Trans. Med. Imag.*, MI-1 , pp.113-119, 1982.

[3] K. Lauckner, "Entwicklung eines iterativen 3D Rekonstruktionsverfahrens für die Kontrolle der Tumorbehandlung mit Schwerionen mittels der Positronen-Emissions-Tomographie", Thesis, Dresden University of Technology, 1999

[4] J.M. Ollinger, „Model based scatter correction for fully 3D PET", *Phys. Med. Biol.*, vol. 41; pp. 153-176, 1996

[5] C.C. Watson et al., „Evaluation of Simulation-Based Scatter Correction for 3-D PET Cardic Imaging", *IEEE Trans. Nuc. Sci.*, vol. 44, no. 1, pp. 90-97, 1997